Controlled Natural Gas Release Experiment in a Confined Aquifer, Northeastern British Columbia (NTS 094A/04): Activity Report 2018–2019

A.G. Cahill, The Lyell Centre, Heriot-Watt University, Edinburgh, Scotland

B. Ladd, The University of British Columbia, Vancouver, British Columbia

J. Chao, The University of British Columbia, Vancouver, British Columbia

J. Soares, The University of British Columbia, Vancouver, British Columbia

T. Cary, University of Calgary, Calgary, Alberta

N. Finke, The University of British Columbia, Vancouver, British Columbia

C. Manning, The University of British Columbia, Vancouver, British Columbia

A.L. Popp, Swiss Federal Institute of Technology and Swiss Federal Institute of Aquatic Science and Technology, Switzerland

C. Chopra, The University of British Columbia, Vancouver, British Columbia

K.U. Mayer, The University of British Columbia, Vancouver, British Columbia

A. Black, The University of British Columbia, Vancouver, British Columbia

R. Lauer, University of Calgary, Calgary, Alberta

C. van Geloven, British Columbia Ministry of Forests, Lands, Natural Resource Operations and Rural Development, Prince George, British Columbia

L. Welch, British Columbia Oil and Gas Commission, Kelowna, British Columbia

S. Crowe, The University of British Columbia, Vancouver, British Columbia

B. Mayer, University of Calgary, Calgary, Alberta

R.D. Beckie, The University of British Columbia, Vancouver, British Columbia, rbeckie@eoas.ubc.ca

Cahill, A.G., Ladd, B., Chao, J., Soares, J., Cary, T., Finke, N., Manning, C., Popp, A.L., Chopra, C., Mayer, K.U., Black, A., Lauer, R., van Geloven, C., Welch, L., Crowe, S., Mayer, B. and Beckie, R.D. (2020): Controlled natural gas release experiment in a confined aquifer, northeastern British Columbia (NTS 094A/04): activity report 2018–2019; *in* Geoscience BC Summary of Activities 2019, Geoscience BC, Report 2020-02, p. 145–160.

Introduction

This paper summarizes the past twelve months of a research program aimed at advancing knowledge on fugitive natural gas migration in groundwater. Research activities were carried out at the Hudson's Hope Field Research Station (HHFRS) located in northeastern British Columbia (BC; Figure 1). In the summer of 2018, natural gas was intentionally injected into the subsurface; the physical and biogeochemical conditions associated with this injection have been monitored ever since. The installation of HHFRS and previous activities at the site are described in Cahill et al. (2019a, b).

This publication is also available, free of charge, as colour digital files in Adobe Acrobat® PDF format from the Geoscience BC website: http://www.geosciencebc.com/updates/summary-of-activities/.

Fugitive gas (FG) describes natural gas that has been unintentionally released in the subsurface in the context of energy resource development. Gas migration (GM) occurs when fugitive gas is released in the subsurface outside of an energy well casing and into the adjacent formation(s), as opposed to fugitive gas that leaks inside the well casing and manifests as surface casing vent flow (SCVF). Although both FG and GM were identified long ago (Chafin, 1994; Dusseault et al., 2000), significant knowledge gaps regarding gas migration, environmental impacts and environmental fate still exist, largely because of the complexity of the physical and biogeochemical processes involved, but also due to the distinct geological environments of the various resource plays. Consequently, there is a pressing need to address knowledge gaps related to FG and GM in northeastern BC, particularly in light of the technological improvements in unconventional production methods in the

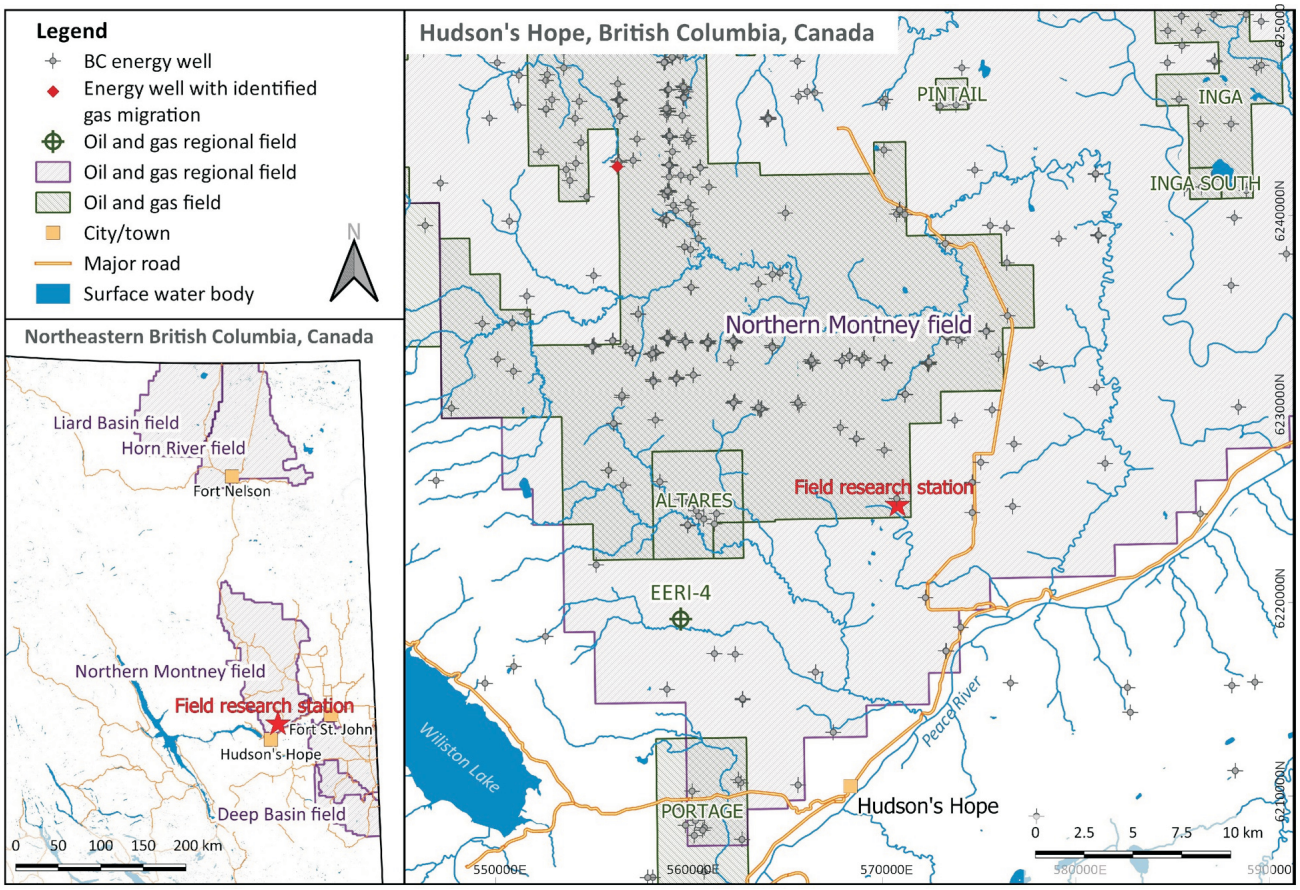

Figure 1. Location of the Hudson's Hope Field Research Station in the context of oil and gas activity in northeastern British Columbia (Cahill et al., 2019a). Co-ordinates are in NAD83 BC Albers. Well locations retrieved from AccuMap™ (IHS Markit, 2019). Oil and gas regional fields and base map features retrieved from DataBC (2019a–d).

last decade and the accompanying increase in exploration and development of petroleum resources (Council of Canadian Academies, 2014). A principal objective of this research program, and the Energy and Environment Research Initiative (EERI) at The University of British Columbia (UBC), is to provide the science knowledge base that can be used to inform the management of oil and gas development in BC. By conducting a controlled natural gas release experiment in an area of active oil and gas development, the aim is to 1) characterize the physical and biogeochemical processes that control subsurface gas migration and impact, and quantify the amount of natural gas that remains, degrades or leaves the subsurface; 2) test FG monitoring and detection methodologies; and 3) inform regulations to facilitate safe and sustainable development of natural gas resources.

Background

Subsurface Gas Movement Fundamentals

In the subsurface, natural gas can move in a gas phase, sometimes called a free-phase gas, or as a dissolved component in groundwater. The GM in the subsurface is therefore governed by multiphase (gas phase and liquid phase) flow and transport, which are controlled by the complex physics and chemistry of the two fluids and the porous media (Parker, 1989; Mercer and Cohen, 1990). Below the water table, free-phase gas will move principally in response to buoyancy and viscosity forces, whereas dissolved gas will move as a solute with groundwater flow, which is controlled by the hydrogeological conditions at a given site (i.e., recharge area locations, topography, etc.). Free-phase gas is subjected to vertical buoyancy forces that will induce vertical movement toward the surface unless intercepted by low-permeability strata such that entry into pore space is inhibited. If not intercepted, free-phase gas will advance from the saturated zone and enter the vadose zone, where, following any degradation processes, it will emit to atmosphere.

The process by which free-phase gas moves, that is, enters into a pore space originally occupied by a liquid, is controlled by the pressure difference between the gas phase and the adjacent liquid phase. This difference in pressure between the phases is called the capillary pressure, which is controlled by the properties of the gas, liquid, geological materials and the pore sizes of the material. For the gas to enter pores that are occupied by liquid, the gas must dis-

place or 'push' the liquid out. It can do this if the capillary pressure is greater than the pressure required to displace the liquid, called the gas-entry pressure.

These free-phase gas dynamics allow a general statement to be made about where to find free-phase gas in the subsurface: because gas-entry pressures are lower for larger pores (Berg, 1975), the free-phase gas will tend to occupy and move through the larger pores and/or fractures in the subsurface. Conversely, free-phase gas movement will be inhibited by materials with smaller pore sizes, which typically have low permeability and require higher entry pressures to advance. The materials or strata that inhibit gas entry into their pore space are called capillary breaks or capillary barriers. With this background, a simple conceptual description of the physical transport of gas in the subsurface can be introduced that will apply at this field research station. This will be followed by a conceptual description of the associated biogeochemical processes in the subsurface.

Conceptual Model of Free-Phase Gas and Dissolved Gas Flow and Transport

The upward flow of free-phase gas below the water table in the subsurface is similar to the downward flow of a dense liquid through a less dense liquid. If a dense liquid is poured into water in a tank, it will move vertically downward until it encounters the bottom of the tank, where the denser liquid will pool and then spread horizontally along the tank bottom. If the tank bottom is not horizontal, the denser liquid will move downslope by gravity along the tank bottom. If there is a local depression, the denser liquid will pool and become trapped in the depression. These same ideas apply for a free-phase gas except that buoyancy forces act vertically upward as opposed to downward. A free-phase gas issuing from a source below the water table will move vertically upward until it encounters a capillary break, where it will pool and spread, and move upslope if the surface of the capillary break material (e.g., a silt or clay) is not horizontal, or pool and become trapped if there is a local convex impression in the bottom of the strata. Examples of this can be found in air-sparging literature, which describes when air is injected into the subsurface to enhance the removal of volatile contaminants (Ji et al., 1993).

If while moving along the bottom of the capillary-break surface, the gas encounters pores or fractures that are sufficiently large for the prevailing capillary pressures, the gas will enter the large pore or fracture and move upward. The gas pool under the capillary break will then be able to 'drain' upward until it either encounters another capillary break, or it crosses the water table. Larger pores, coarser materials and wider fractures are therefore important preferential flow paths for free-gas movement in the subsurface.

A key question for a given site where gas is leaking at some depth into the subsurface is whether that gas can cross the water table and enter into the near-surface pore space that is connected to the atmosphere in the vadose zone. If so, it can then be emitted through the unsaturated subsurface and reach the atmosphere, where methane acts as a greenhouse gas (Forde et al., 2019a).

Natural gas can also move with groundwater as a dissolved gas. The hydrogeology of the subsurface controls groundwater flow directions, magnitudes and velocities, whereas the total flux of dissolved gas that can be transported in groundwater depends upon the amount of gas that can dissolve and the groundwater flow rate. The amount of gas that can dissolve per unit volume of water at equilibrium increases with water pressure (the dissolution of carbon dioxide is also affected by pH) and to a lesser degree temperature. Generally speaking, deeper groundwater has higher water pressure (and in general temperatures) and accordingly can dissolve more gas. The rate at which gas dissolves will depend strongly on the surface-to-volume ratio of the free-phase gas and the rate at which water flows by the free-phase gas zones in the subsurface. Gas will dissolve into water more readily if the free-phase gas has a relatively large surface area, and the water flow past the free-phase gas is relatively fast.

The principal biogeochemical process that affects GM in the subsurface is oxidation of methane. With the exception of explosive conditions, methane oxidation is kinetic; that is, it does not occur instantaneously, but at rates that depend upon biogeochemical conditions and temperature. Fundamentally, oxidation is a transfer of electrons from the carbon in methane to an electron acceptor such as oxygen. Generally speaking, bacteria in the subsurface mediate many, if not most, of the oxidation reactions for their respiration (Lovley and Chapelle, 1995). Bacteria can 'burn' methane by 'breathing' oxygen, creating carbon dioxide and water. Other dissolved and mineral phases can also serve as electron acceptors, most notably dissolved nitrate and sulphate and solid oxide mineral phases, principally of iron and manganese (Christensen et al., 2001). Methane can be oxidized in absence of oxygen in the subsurface in a process called anaerobic oxidation, affecting the concentrations of nitrate, sulphate and iron dissolved in water and generating several byproducts including hydrogen sulphide and trace metals such as arsenic (Forde et al., 2019b).

An important question is if, and how quickly, will methane in natural gas oxidize in the subsurface. Most often, oxidation in the presence of oxygen is faster than anaerobic oxidation, and oxidation at higher temperatures is faster than at lower temperatures (Appelo and Postma, 2005). This suggests that oxidation of methane in groundwater or in the soil gas will be more rapid near the surface where oxygen is more likely to be present, and in the summer when tempera-

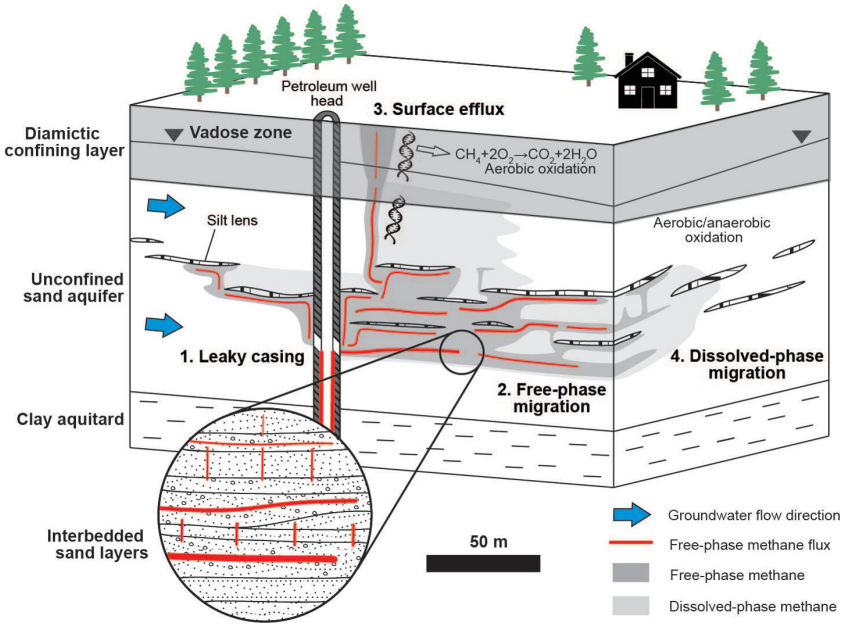

Figure 2. Conceptual model of gas migration and fugitive gas associated with energy wells (modified from Cahill et al., 2017). Fugitive gas may affect the saturated zone (below the water table), the unsaturated zone (with a gas phase connected to the atmosphere) and the atmosphere. Gas moves vertically but can be directed laterally along capillary breaks such as silt or clay layers.

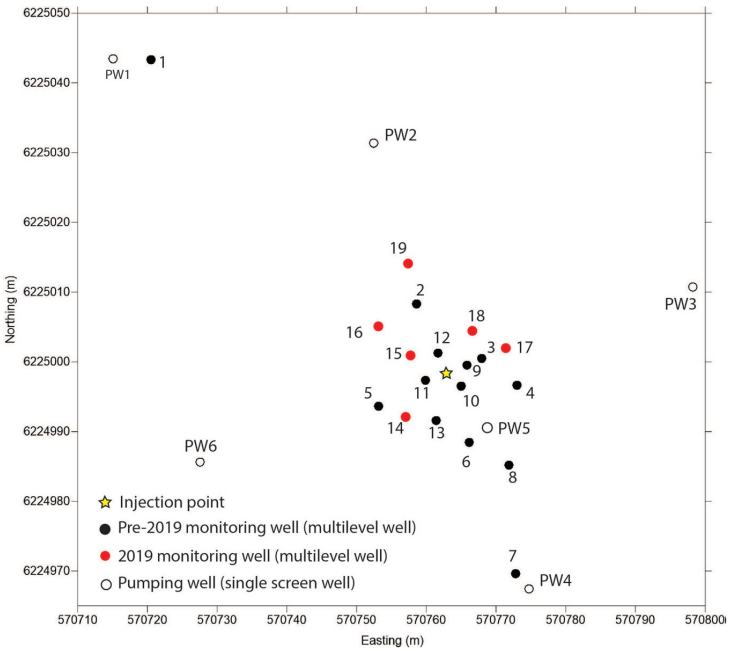

Figure 3. Surface location of monitoring wells in the study area as of October 2019.

tures are higher. These processes are summarized in Cahill et al. (2017) and shown in Figure 2.

These physical and biogeochemical processes depend upon the prevailing subsurface properties such as grain size, distribution of capillary breaks and large pores/channels, subsurface mineralogy and geochemistry, and are best investigated through an experimental program. At the HHFRS, a leak of gas from a point source in the subsurface was emulated and its physical movement and geochemical effects on groundwater and rates of emission to the atmosphere are being monitored. Research activities over the last twelve months at HHFRS are described below. These build on previous efforts, described in Cahill et al. (2019b).

Summary of Activities and Progress

Saturated Zone Injection Experiment

At HHFRS, an active controlled natural-gas injection period lasted 66 days, during June to August 2018. From fall 2018 to present, efforts have focused on characterization and monitoring of groundwater quality, flow conditions, surface effluxes, gas compositions and changes in geophysical conditions.

To better constrain the sedimentary architecture at HHFRS following observations of gas migration, a total of 15 new sampling ports in six nested wells were added to the groundwater monitoring well network in September 2019 (Figure 3). Boreholes were drilled by sonic method allowing core to be logged, intact sediment samples to be collected for characterization of permeability, analysis of gas in sediments via ISOPAK™ containers from Isotech Laboratories, Inc., and collection of samples for incubation studies to characterize microbial activity. The new sampling wells were installed with 5 cm (2 in.) diameter screens to facilitate groundwater collection with displacement pumps, particularly beneficial for points completed in lower permeability materials.

Discipline-Specific Activities

Hydrogeology and Groundwater Monitoring

Physical and geochemical properties of groundwater and dissolved gas have been monitored from May 2018 to present (October 2019). Groundwater samples were collected approximately monthly, with the exception of winter months, from the pre-September 2019 sampling points, which include sample ports in 13 multilevel monitoring wells and from six single-depth screened piezometers (see Table 1). In the field, temperature, specific conductance and pH were measured using probes installed in flow-through cells. Alkalinity was determined onsite by Gran titration of filtered samples. Trace

Table 1. Completion details for installed nested sampling wells, as of September 2019. Abbreviations: MW, monitoring well; PW, pumping well.

Pre-2019 wells			
Well ID	Sampling port	Completion intervals from (m)	to (m)
PW1	N/a	23.2	26.2
PW2	N/a	22.3	25.3
PW3	N/a	22.3	25.3
PW4	N/a	19.8	22.9
PW5	N/a	18.5	20.0
PW6	N/a	15.8	25.0
MW1	2	16.0	16.6
MW2	1	11.6	12.5
	2	14.6	15.8
	3	18.9	19.6
MW3	2	14.6	15.5
MW4	1	11.6	12.2
	2	14.6	15.2
	3	16.8	17.7
	4	19.5	20.1
MW5	2	16.9	17.5
	3	19.2	19.8
	4	21.0	21.6
MW6	1	11.9	15.5
	2	15.8	16.7
	3	18.0	18.6
	4	20.1	20.7
MW7	1	11.9	12.5
	2	14.9	15.5
	3	17.1	17.7
	4	20.1	20.7
MW8	1	12.0	12.6
	2	16.0	16.6
	3	18.0	18.6
	4	20.0	20.6
MW9	3	18.0	18.6
	4	20.0	20.6
MW10	1	12.0	12.6
	2	16.0	16.6
	3	18.0	18.6
	4	20.0	20.6
MW11	1	12.0	12.6
	3	18.0	18.6
	4	20.0	20.6
MW12	1	12.0	12.6
	2	16.0	16.6
	3	18.0	18.6
	4	20.0	20.6
MW13	1	12.0	12.6
	3	18.0	18.6
	4	20.0	20.6

2019 wells			
Well ID	Sampling port	Completion intervals from (m)	to (m)
MW14	1	8.5	9.1
	2	11.3	11.9
	3	16.8	18.3
MW15	1	14.3	14.9
	2	17.4	18.9
MW16	1	11.3	11.9
	2	15.8	16.5
	3	18.3	18.9
MW17	1	11.3	11.9
	2	18.6	19.2
MW18	1	11.3	11.9
	2	16.8	17.4
MW19	1	11.3	11.9
	2	15.5	16.2
	3	17.7	18.3

elements were analyzed at the Water Quality Centre at Trent University (Peterborough, ON) using inductively coupled plasma–mass spectrometry. Anion concentrations in groundwater samples were determined by ion chromatography and automated colourimetry at the Applied Geochemistry group (AGg) Chemistry Lab at the University of Calgary (Calgary, AB). Dissolved gas composition for N_2, O_2, CO_2 and C_1 to C_3 (methane to propane) was analyzed using a Bruker 450 gas chromatograph at the AGg Chemistry Lab.

During the injection period, two wells (MW2, MW5) showed elevated dissolved methane concentrations compared to background levels (Table 2). Well MW2 exhibited particularly high dissolved methane concentrations (12.27 and 15.78 mg/L at ports 2 and 3, respectively), whereas MW5 showed more modest increases to 0.25 and 0.1 mg/L at ports 3 and 4, respectively. As can be seen in Figure 3, MW2 and MW5 are not the most proximal wells to the injection point, nor to each other, indicating that gas migration is largely controlled by small-scale geology and discrete preferential pathways. Approximately 44 days after the active injection of natural gas stopped (day 110), evidence of injected gas was detected in the dissolved phase in an additional two wells (MW11, MW12) and an additional shallower port in MW2. In the most recent results from September 2019 (day 460), two more wells (MW9, MW13) showed elevated dissolved methane in multiple ports, whereas MW5 decreased back down to background levels. In general, the highest methane concentrations have been observed in the shallower sample ports. Overall, preliminary mass balance calculations indicate that the majority of the injected gas has remained in the free-phase gas form, with a small proportion dissolving into the groundwater. Over a year since the start of the injection, it is clear the groundwater chemistry is still evolving.

Since June 6, 2018, hydraulic heads have been recorded by pressure transducers at MW6 at 12 and 20 m depth, MW13 at 15 m depth and MW10 at 16 m depth. These data will be

Table 2. Dissolved methane (CH_4) gas concentrations for wells and sampling ports that showed elevated concentrations at some point during the experiment. Dissolved methane concentrations are shown for days –6, 60, 110 and 460, with day 0 being the day the injection began. The active injection lasted for 66 days. Elevated concentrations from background are highlighted in bold. Abbreviation: N/d, no data, due to low or nonexistent flow.

Well ID	Sampling port	Depth (top of interval) (m)	Before injection (day -6) CH_4 (mg/L)	During injection (day 60) CH_4 (mg/L)	Post injection (day 110) CH_4 (mg/L)	Post injection (day 460) CH_4 (mg/L)
MW2	1	11.6	0.0019	ND	**9.75**	**7.09**
	2	14.6	0.0017	**12.27**	**13.18**	N//d
	3	18.9	0.0021	**15.78**	**14.15**	**14.30**
MW5	3	19.2	0.0021	**0.25**	**0.100**	0.0028
	4	21.0	0.0037	**0.1000**	**0.111**	N/d
MW9	3	18.0	0.0039	0.0065	0.0058	**10.60**
	4	20.0	0.0250	0.0159	0.0093	**0.47**
MW11	1	12.0	0.0030	0.0088	**0.1114**	**0.253**
	3	18.0	0.0230	0.0050	0.0131	**0.11**
	4	20.0	0.0168	0.0123	0.0127	**0.82**
MW12	2	16.0	0.0017	0.0181	0.0166	**10.032**
	4	20.0	0.0056	0.0091	**0.0231**[(1)]	**0.598**
MW13	3	18.0	0.0035	0.0110	0.0032	**0.370**

[(1)] Highlighted because even though the CH_4 level is low, other dissolved constituents showed evidence of injection gas.

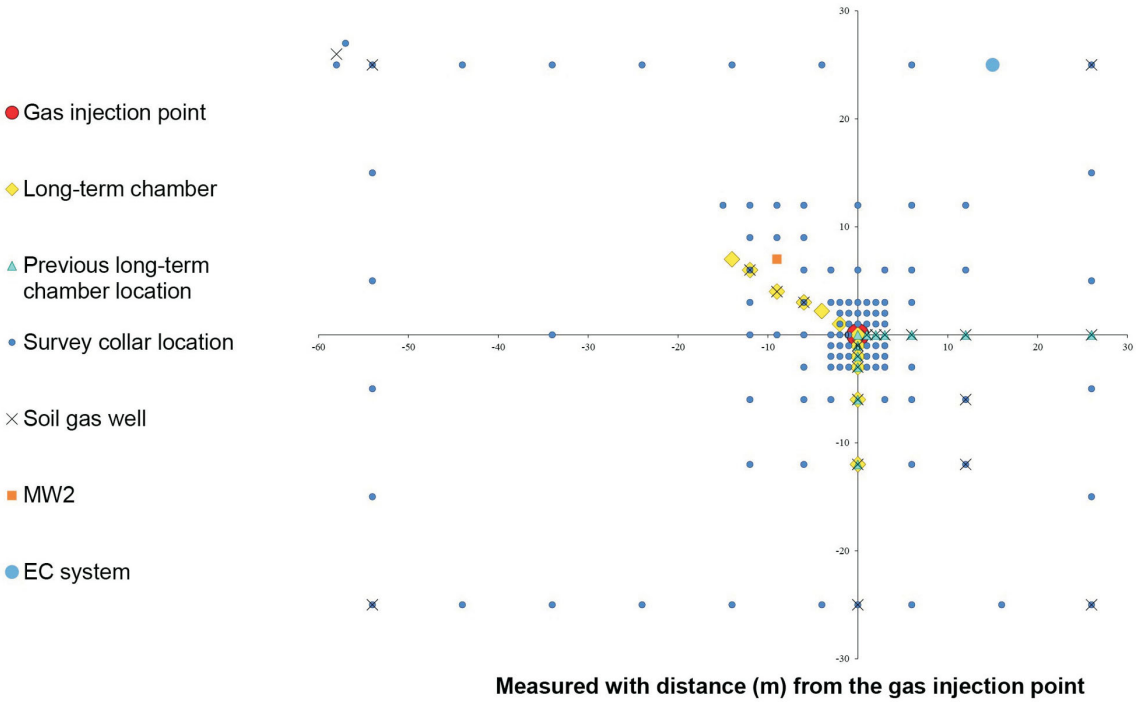

Figure 4. Illustration of the experimental setup and monitoring network for the vadose zone and surface efflux measurements at the Hudson's Hope Field Research Station. Abbreviations: EC, eddy covariance; MW, monitoring well.

compared to data from air-sparging studies (Johnson et al., 2001) where subtle transient pressure responses have been observed in groundwater levels and used to interpret groundwater flow directions and to infer gas movement.

Soil Gas and Surface Efflux

To monitor soil-gas concentrations and surface effluxes, 12 dynamic long-term chambers (8100-104, LI-COR, Inc.) were deployed and 22 soil-gas sampling ports were installed at HHFRS, primarily along two transects radiating from the injection point (Figure 4). The 12 long-term dynamic chambers sequentially measured carbon dioxide and methane concentrations at their designated locations. This allowed for the calculation of fluxes at the surface and provided high-resolution time series data for methane fluxes. The 22 soil-gas sampling locations were manually augured with sampling ports at 0.45 and 1.15 m below ground surface, allowing for the collection of soil-gas samples for compositional and isotope analyses. Additionally, 105 survey collars (green rings in Figure 5) were set up and an additional set of analyzers allowed for carbon dioxide and methane concentrations to be obtained across the site, providing discrete, detailed, spatially distributed, flux data. Survey flux measurements and soil-gas samples for isoto-

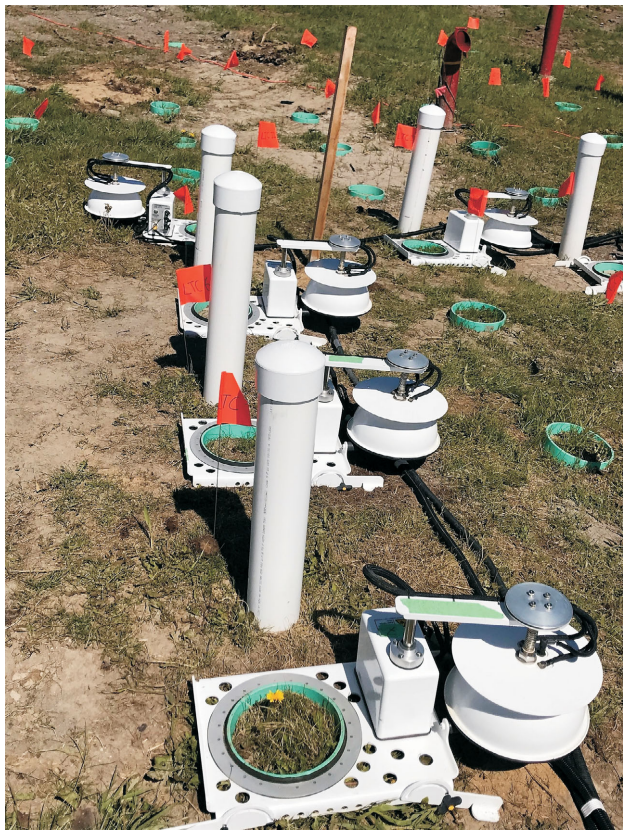

Figure 5. Dynamic long-term chambers sitting on green collars and co-located with soil-gas wells with white polyvinyl chloride (PVC) protective casings.

Figure 6. Operation of the miniRUEDI at Hudson's Hope Field Research Station.

pic and compositional analysis were collected every 2–4 weeks starting on May 28, 2018, ending on October 1, 2018, at the onset of winter conditions. Additionally, soil-gas samples were collected once in June 2019. The results illustrate that the injected gas moved upgradient against groundwater flow and broke through at the surface a month after the injection. Once the gas was detected, elevated methane (CH_4) fluxes were continuously detected at the surface and began to decrease exponentially after the injection was stopped. Soil-gas composition and isotopic data further show evidence that the injected gas moved through the near subsurface to surface and that CH_4 was microbially oxidized to CO_2.

Application of the miniRUEDI Portable Mass Spectrometer at HHFRS

During the HHFRS injection experiment, instruments were installed that provided continuous real-time measurements of surface emissions of the injected gas (soil efflux chamber and an eddy covariance flux tower, the latter discussed in the following section). While planning for the HHFRS injection experiment, novel field-portable methods were investigated for real-time detection of the injected gas in the subsurface, as the soil-gas and groundwater samples collected in vials take approximately one month to analyze. The portable mass spectrometer system selected was Gasometrix GmbH's miniRUEDI (Brennwald et al., 2016), developed by scientists at the Swiss Federal Institute for Aquatic Science and Technology (Figure 6).

It was decided to use the miniRUEDI during and following the controlled release experiment to achieve two scientific goals: 1) to provide real-time detection of the injected gas in the subsurface and 2) to provide measurements of He concentration. The miniRUEDI has the ability to detect a wide range of gases (including He, Ar, Kr, N_2, O_2, CO_2, CH_4, C_3H_8). The injected gas contained 5000 ppm He (1000 times higher than the atmospheric concentration of 5 ppm), but this gas could not be measured by the instrument used for the discrete soil-gas and groundwater samples. Helium is a particularly useful tracer because it is not produced or consumed by any biological or chemical process. Therefore, changes in the ratio of helium to hydrocarbons can provide insights into the subsurface consumption of the injected hydrocarbons.

The miniRUEDI was used at the HHFRS prior to, during and following the injection (in June, July and August 2018). In late July 2018, approximately five weeks after the injection began, the miniRUEDI detected elevated levels of tracer gases (methane, propane, helium) at MW2 (Figure 2). At MW2, groundwater was sampled and it was found that the peak heights for CH_4 and He were approximately 1000 times higher than the levels in air or air-equilibrated water. Subsequent measurements of soil efflux adjacent to MW2 also showed elevated levels of CH_4. As a result, the location of one of the soil efflux chamber long-term monitoring lines was moved so that it was close to MW2. The chambers closest to MW2 displayed much higher CH_4 levels than anywhere else on the site, and these data were necessary to accurately estimate the CH_4 emissions.

Following soil-gas composition measurements in the laboratory, the miniRUEDI was used to measure selected samples. All soil-gas samples that contained detectable levels

of tracer gas also contained elevated levels of He. Further interpretation of the miniRUEDI data will be presented in upcoming peer-reviewed publications.

Overall, the miniRUEDI was a highly successful component of the experiment. The real-time detection of the injected gas at MW2 enabled the modification of the monitoring strategy during the experiment, improving estimates of the surface efflux. Additionally, a collaboration with European researchers was developed that will expand the international visibility of this research.

Eddy Covariance and Micrometeorology

The eddy covariance (EC) system was re-installed in March 2019, after the 2018–2019 winter decommissioning, with two main objectives:

1) to monitor any residual effluxes during and after the thaw,
2) to carry out controlled release experiments to evaluate flux footprints.

The system was set up similar to 2018 (Cahill et al., 2019b), however, the height of the tower was raised to 1.9 m to expand the flux footprint (Figure 7). All instruments as used in the previous year were re-installed, i.e., a 3-D sonic anemometer (CSAT3B, Campbell Scientific, Inc.), which measures wind direction and speed in three dimensions; a gas analyzer (LI-7700, LI-COR, Inc.) for methane, which is an open path system; and a gas analyzer (LI-7200, LI-COR, Inc.) for carbon dioxide and water vapour, which is an enclosed unit with a flow module. There is also a flow module (7200-101) with the LI-7200, which is responsible for maintaining a precise and controllable flow of air. An LI-7550 analyzer interface unit (AIU) was set up, which integrates data from the sonic anemometer and the LI-7200 and LI-7700 analyzers. The SmartFlux 2 system by LI-COR, powered by their EddyPro® software, was also installed. It computes covariances from the 20 Hz high frequency raw values (mixing ratios, wind velocity, etc.) obtained from the gas analyzers and provides half hourly averages for this data.

Figure 7. Eddy covariance system configuration at Hudson's Hope Field Research Station.

The climate system was also re-installed, including a net radiometer (CNR4, Kipp & Zonen B.V.); a 2-D anemometer (Windsonic, Gill Instruments Limited); CSI sensors (manufactured by Vaisala Corporation) for barometric pressure (CS106), temperature and relative humidity (HMP155A); three Decagon Devices, Inc. GS3 sensors (each measuring soil moisture, soil conductivity, soil temperature); two soil heat flux plates (HFP01-L, HFP01SC-L, Hukseflux Thermal Sensors B.V.) at a depth of 5 cm each, the latter being self-calibrating; and a tipping bucket rain gauge (TE525WS, Texas Electronics, Inc.).

A datalogger (CR1000, Campbell Scientific, Inc.) at the site collected all the climate data from the various components, and compiled it giving the averages, maximum and minimum values of each parameter every half hour. This climate data, after being collected onto the datalogger, and along with the computed EC measurements (by the Smartflux 2) were remotely sent to the UBC Biometeorology Soil and Physics Group lab daily at 6 a.m. via a modem (RV50, Sierra Wireless S.A.). The high-frequency data was collected onto a USB at the site and sent back and forth between the site and UBC.

Controlled atmospheric-release experiments were carried out in the summer of 2019 (Table 3), to study the response of EC measurements to factors like release rate, release location, release height and distance with respect to the tower. The objective was to fill in knowledge gaps about the footprint, i.e., the relationship between surface effluxes and EC measurements made at the EC tower. Based on this theory, relationships between EC fluxes and chamber measurements can be drawn (analysis in progress). Various footprint models (e.g., Kormann and Meixner, 2001; Kljun et al., 2015) can be used to do this analysis, depending on experimental conditions such as release height, stability parameters of the atmosphere, etc. The decision of which footprint model to use will be made by using data from these release experiments.

Table 3. Timeline of fieldwork in 2019 at Hudson's Hope Field Research Station.

Date of trip	Purpose
March 19 to 22	Re-installation of eddy covariance system
May 13 to 17	Surface release experiment
July 15 to 22	Surface release experiment
August 12 to 15	Surface release experiment (repeated some July experiments to have more confidence in measurements)

Various approaches were determined to compare flux data from the EC system with that from the chambers (including data from 2017 and 2018). In order to test this theory, EC fluxes were estimated using the release rate of the source and the footprint value at the location of the source, and these estimates were compared with actual measured EC fluxes. This was done for a release experiment conducted in 2017, and the results were very promising (Figure 8; C. Chopra, work in progress).

Similar analysis is in progress for the releases from this summer (2019) and this information will further be utilized to 1) make direct comparison with the data from chambers by combining chamber effluxes with the flux footprint, and 2) obtain the surface distribution of effluxes using EC fluxes and the flux footprint by carrying out a matrix inversion.

Geophysics

The geophysics team visited the site in late June 2019 to conduct a final post-injection electrical resistivity survey (Figure 9). The data collection employed the same configuration used in the previous surveys, which were designed to map the migration of the gas through time-lapse analysis

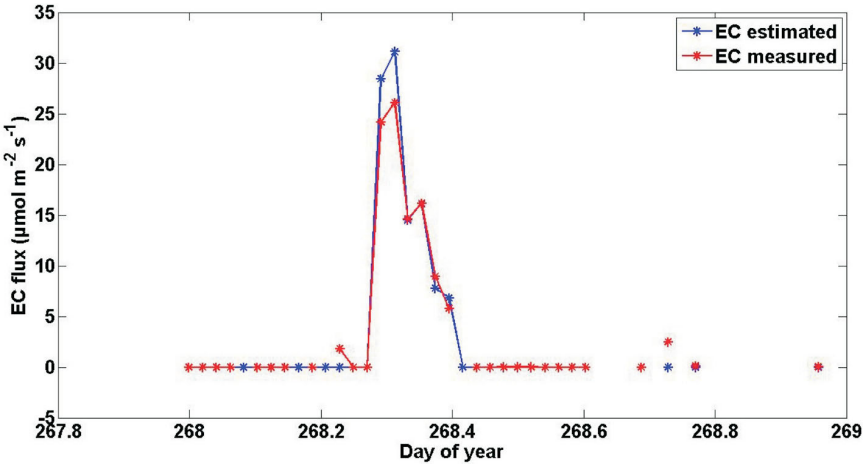

Figure 8. Estimated versus measured values of eddy covariance (EC) flux from the 2017 surface release experiment.

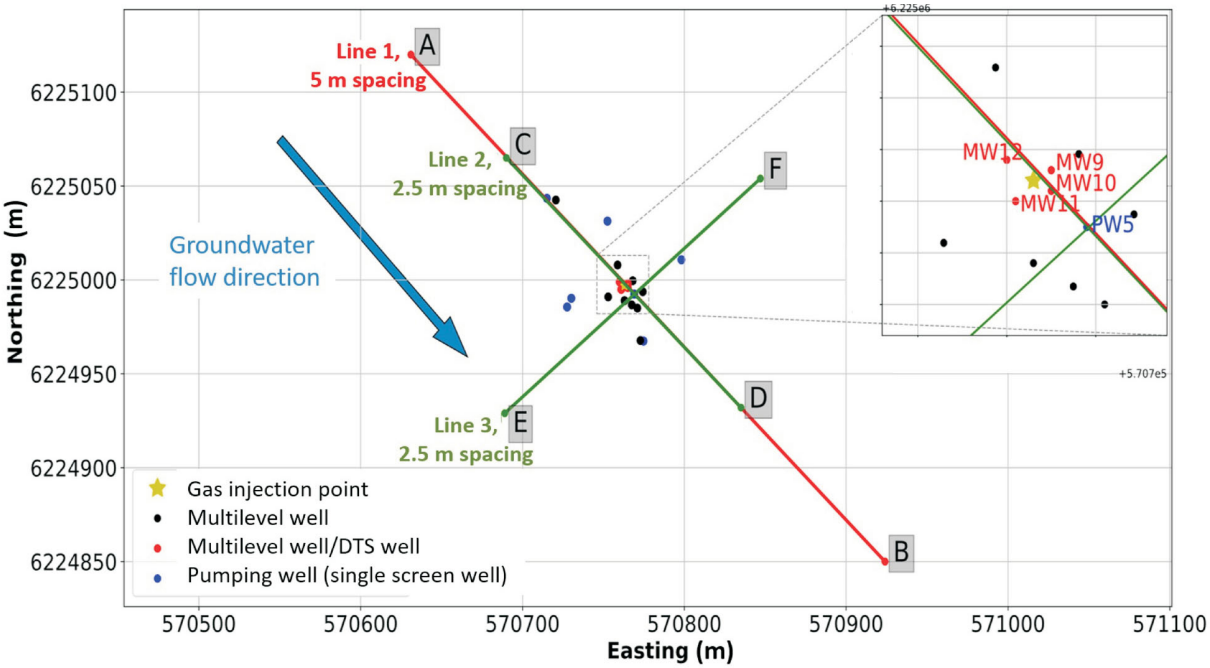

Figure 9. Site map showing the orientation of three electrical resistivity profiles measured across two line transects: line 1 consists of two survey lines, AB (5 m spacing of electrodes) and CD (2.5 m spacing of electrodes), and line 3 consists of one survey line, EF (2.5 m spacing of electrodes). The injection point is located at the centre of line CD. Wells MW9, MW10, MW11 and MW12 contain optical fibre for distributed temperature sensing (DTS) measurements, which were used to calculate temperature corrections for resistivity measurements.

(Cahill et al., 2019b). Two additional resistivity lines were collected around MW2 in an effort to identify potential sites of leakage, or gaps in the confining layer, which represent pathways for gas migration (Figure 10). Analysis of the time-lapse data is complete, and a manuscript is being prepared for submission to a peer-reviewed journal. The preliminary results were presented at the annual American Geophysical Union (AGU) Fall Meeting in Washington, DC, in December 2018 (Cary et al., 2018).

Microbiology

Sampling

Just prior to the start of the injection on June 12, 2018, all wells were sampled for H_2S, microbial diversity, cell counts, single cell amplified genomes, methane oxidation, methanogenesis and sulphate reduction (Tables 4, 5). Wells MW2, MW7 and MW10 were chosen for microbial rate determinations, with MW2 being upstream of the well (potentially a control) and MW7 and MW10 being downstream at varying distances. Following the injection, sampling was focused on the wells surrounding the injection point, collected about every two weeks. Low temperatures in late September 2018 prevented sampling during that month. After September 2018, the number of samples increased to cover the wells where methane had been discovered as well as the two inner circles of wells surrounding the injection well as to not miss wells where the gas may have been migrating (Table 4).

In September 2019, an additional drilling campaign was performed to get a better understanding of the gas plume in three dimensions as well as to obtain contamination control samples, soil samples for rates of microbial transformation of methane and sulphate reduction, and microbial diversity data from groundwater samples to compare with in situ microbial community determined from core samples. Six additional cores (MW14–MW19) were drilled and 15 sampling ports were installed. Soil samples were taken from four to seven horizons from each core (Table 6). Due to time constraints and late development of the new wells, no water samples from the new wells were taken during that trip. These will be sampled during the final sampling campaign in mid-October 2019. Results were not available for this publication.

Analysis

Incubation rates are determined by either radio tracer (sulphate reduction rate [SRR], methanogenesis [Met], dark carbon fixation [DCF]) or time course incubations (aerobic methane oxidation [MOX]) just after returning from the field site. First samples were analyzed for SRR, MOX and DCF rates. Following the September drilling campaign, soil rates were determined in MW15 at 12.2 m (40 ft.), 15.2 m (50 ft.) and 18.6 m (61 ft.), MW16 at 15.2 m (50 ft.) and MW19 at 12.2 m (40 ft.) and 18.3 m (60 ft.). Well MW15 at 18.6 m (61 ft.) showed the highest methane reading of 10% lower explosive limit (LEL) in the pumped water. Using an RKI Instruments, Inc. Eagle 2 gas monitor, testing for methane revealed methane was not detected at the other depths in MW15 and MW16. Wells MW17, MW18 and MW19 were not tested on site for methane.

Samples from the injection well and the monitoring and pumping wells collected prior to injection have been analyzed for total microbial community composition (Figure 11).

The new sampling method to determine in situ microbial diversity of an aquifer from water samples is based on analyzing the extracellular DNA (eDNA) in the water. To validate the method, the eDNA in the water samples must be analyzed along with the eDNA and intracellular DNA (iDNA) of the soil samples. For this project, a method has been developed to separate the eDNA and iDNA in both the water samples and the soil samples. This work is currently underway.

Preliminary Results

The microbial diversity in the water samples collected prior to injection show a clear difference in microbial composition and abundance between the pumping wells and the monitoring wells. This is most likely due to the longer screens in the pumping wells and thus mixing of water from different horizons. The pumping wells, however, also show a bigger variation in the abundance of microbes than in the

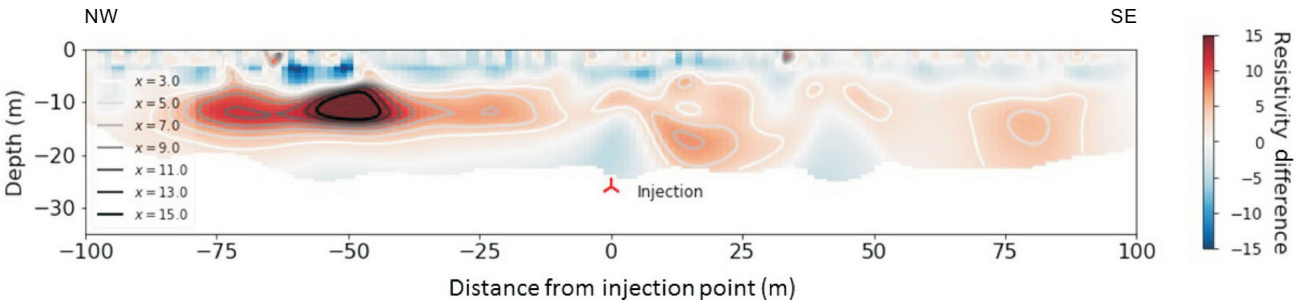

Figure 10. Images of percentage difference in resistivity for the time-lapse inversions of line 1 (survey line CD; 2.5 m electrode spacing), relative to pre-injection conditions. Grayscale contour lines (x-values on left axis) emphasize the resistivity difference gradient (red–blue colours) along transect CD. Line 1 is oriented parallel to the groundwater flow direction (see Figure 9). Abbreviations: NW, northwest; SE, southeast.

Table 4. Samples taken for microbial diversity, cell counts and single amplified genomes. The "s" denotes that S-isotope samples were also taken. Abbreviation: Inj, injection point.

Well ID - sampling port	October 17, 2017	June 6–12, 2018	June 27–28, 2018	July 12, 2018	July 27, 2018	July 30, 2018	August 15, 2018	August 27, 2018	September 18–19, 2018	October 5, 2018	October 29–31, 2018	May 5, 2019	July 19–20, 2019	September 9–12, 2019
PW1	x	s										x		
PW2	x	s										x		
PW3	x	s										x		
PW4	x	s										x		
PW5	x	s												
PW6	x	s										x		
Inj		x												
MW1-2		s	x	x		x	x	x	x			x	s	
MW2-1		s									x	x	s	
MW2-2		s				x	x	x	x	x				
MW2-3		s				x		x	x	x	x	x	s	s
MW3-2		s			x	x		x	x			x	s	x
MW4-1		s								x	x	x	s	s
MW4-2		s								x	x	x	s	s
MW4-3		s								x	x	x	s	s
MW4-4		s								x	x	x	s	
MW5-2												x		
MW5-3										x	x	x	s	
MW5-4										x				
MW6-1		s								x	x	x	s	s
MW6-2		s								x	x	x	s	s
MW6-3												x	s	s
MW6-4		s								x	x	x	s	s
MW7-1		s									x	x	s	s
MW7-2		s									x	x	s	s
MW7-3		s									x	x	s	s
MW7-4		s									x	x	s	s
MW8-1		s									x	x	s	x
MW8-3												x	s	s
MW8-4		s									x	x	s	s
MW9-3		s	x	x		x	x	x	x		x	x	s	s
MW9-4		s	x	x		x	x	x	x		x	x	s	s
MW10-1											x			
MW10-3		s		x		x	x	x	x					
MW10-4		s		x		x	x	x	x	x	x	x	s	s
MW11-1		s									x	x	s	s
MW11-3		s	x	x		x	x	x	x		x	x	s	s
MW11-4		s									x	x	s	x
MW12-1											x			
MW12-2											x			
MW12-3				x			x	x						
MW12-4		s							x		x	x	s	s
MW13-1											x			
MW13-3											x			
MW13-4		s									x	x	s	

Table 5. Samples taken for sulphate reduction, methanogenesis, methane oxidation and dark carbon fixation rates.

Well ID - sampling port	June 2018	July 2018	August 2018	May 2019	July 2019	September 2019
MW2-1	SRR, Met-H, Met-Ac, MOX	SRR, Met-H, Met-Ac, MOX	SRR, Met-H, Met-Ac, MOX	SRR, Met-H, Met-Ac, MOX, DCF		
MW2-2	SRR, Met-H, Met-Ac, MOX	SRR, Met-H, Met-Ac, MOX	SRR, Met-H, Met-Ac, MOX			
MW2-3	SRR, Met-H, Met-Ac, MOX	SRR, Met-H, Met-Ac, MOX	SRR, Met-H, Met-Ac, MOX	SRR, Met-H, Met-Ac, MOX, DCF	SRR, Met-H, Met-Ac, MOX, DCF	SRR, Met-H, Met-Ac, MOX
MW7-1	SRR, Met-H, Met-Ac, MOX	SRR, Met-H, Met-Ac, MOX	SRR, Met-H, Met-Ac, MOX	SRR, Met-H, Met-Ac, MOX, DCF	SRR, Met-H, Met-Ac, MOX, DCF	
MW7-2	SRR, Met-H, Met-Ac, MOX	SRR, Met-H, Met-Ac, MOX	SRR, Met-H, Met-Ac, MOX	SRR, Met-H, Met-Ac, MOX, DCF	SRR, Met-H, Met-Ac, MOX, DCF	SRR, Met-H, Met-Ac, MOX, DCF
MW7-3	SRR, Met-H, Met-Ac, MOX	SRR, Met-H, Met-Ac, MOX	SRR, Met-H, Met-Ac, MOX	SRR, Met-H, Met-Ac, MOX, DCF	SRR, Met-H, Met-Ac, MOX, DCF	SRR, Met-H, Met-Ac, MOX
MW7-4	SRR, Met-H, Met-Ac, MOX	SRR, Met-H, Met-Ac, MOX	SRR, Met-H, Met-Ac, MOX	SRR, Met-H, Met-Ac, MOX, DCF	SRR, Met-H, Met-Ac, MOX, DCF	SRR, Met-H, Met-Ac, MOX, DCF
MW10-3	SRR, Met-H, Met-Ac, MOX	SRR, Met-H, Met-Ac, MOX	SRR, Met-H, Met-Ac, MOX			
MW10-4	SRR, Met-H, Met-Ac, MOX	SRR, Met-H, Met-Ac, MOX	SRR, Met-H, Met-Ac, MOX	SRR, Met-H, Met-Ac, MOX, DCF	SRR, Met-H, Met-Ac, MOX, DCF	SRR, Met-H, Met-Ac, MOX

Abbreviations: DCF, dark carbon fixation; Met-Ac, acetoclastic methanogenesis; Met-H, hydrogenotrophic methanogenesis; MOX, aerobic methane oxidation; SRR, sulphate reduction rate

Table 6. Soil samples taken during drilling in September 2019.

Well ID	Depth (m)	Depth (ft)	Cell counts	e/iDNA	Total DNA	Rate samples	Contamination control
MW14	9.1	30	x	x	x		
	12.2	40	x	x	x		
	15.2	50	x	x	x		
	18.6	61	x	x	x		
	20.1	66	x	x	x		
MW15	3.0	10	x	x	x		x
	6.1	20	x	x	x		x
	9.1	30	x	x	x	x	x
	12.2	40	x	x	x	x	x
	15.2	50	x	x	x	x	x
	18.6	61	x	x	x	x	x
	20.1	66	x	x	x		x
MW16	9.1	30	x	x	x	x	x
	12.2	40	x	x	x	x	x
	15.2	50	x	x	x	x	x
	18.3	60	x	x	x	x	x
MW17	9.1	30	x	x	x		x
	12.2	40	x	x	x		x
	15.2	50	x	x	x		x
	18.3	60	x	x	x		x
MW18	9.1	30	x	x	x		
	12.2	40	x	x	x	x	
	15.2	50	x	x	x	x	
	18.6	61	x	x	x		
MW19	9.1	30	x	x	x	x	x
	12.2	40	x	x	x	x	x
	15.2	50	x	x	x	x	x
	15.8	52	x	x	x		
	18.3	60	x	x	x	x	x

monitoring wells. This again could be due to the longer screen, which might be sampling horizons that are not covered in the monitoring wells. Additionally, the pumping wells are more prone to contamination and the initial sampling showed a high abundance of cow hair in the samples, indicating surface contamination (HHFRS is located within a grazing lease and, though protected by an electric fence, is susceptible to cow intrusion). Overall, most of the pumping wells cluster away from most of the monitoring wells in a hierarchical cluster analysis.

There was no consistent pattern of microbial diversity found in samples from the monitoring wells, either in terms of sampling depth or well location.

Unsaturated Zone Injection Experiment

As reported in Cahill et al. (2019b), a second injection experiment was carried out at a separate but nearby site to HHFRS where unsaturated conditions exist. This experiment concluded at the end of 2017, with an additional round of soil samples collected in the summer of 2018. The past year saw the completion of analysis and interpretation of data from this site, and the publication of a peer-reviewed manuscript describing the effects of barometric fluctuations on surface effluxes (Forde et al., 2019a). A second manuscript is in preparation, examining the quantification of attenuation capacity of FG in unsaturated soils.

Conclusions and Ongoing Work

The following forms a summary of the progress made to date with respect to The University of British Columbia Energy and Environment Research Initiative's controlled methane release investigation project:

- completion of field activities at the unsaturated-zone site and publication of peer-reviewed manuscript entitled *Barometric-pumping controls fugitive gas emissions from a vadose zone natural gas release* (Forde et al., 2019a);
- continued monitoring, sample collection, geophysical surveying and microbial experiments at the Hudson's Hope Field Research Station;
- installation of 15 additional monitoring wells in six boreholes in September 2019;
- dissemination of work through conferences including GeoConvention, the American Geophysical Union Fall Meeting and The Geological Society of America Annual Meeting.

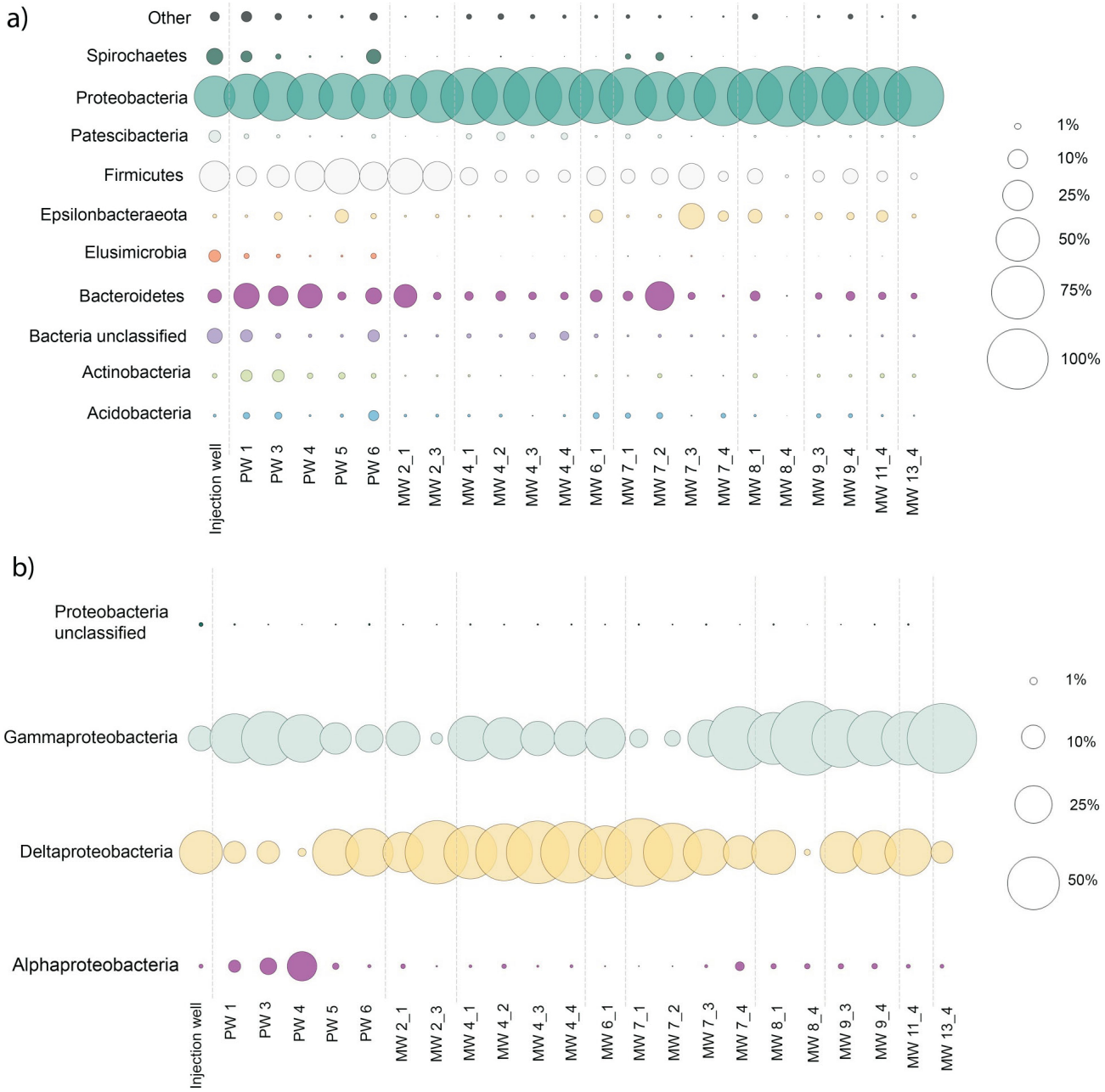

Figure 11. Bubble plot showing **a)** the microbial diversity on a phylum level and **b)** the diversity of proteobacteria in the pre-injection samples. The monitoring well number is followed by the sampling port number.

The bulk of future work on this project will be directed at data interpretation and analysis with mechanistic models. Final data collection will comprise several more rounds of groundwater sampling in order to capture the evolution of groundwater quality and gas dynamics through time at Hudson's Hope Field Research Station.

Acknowledgments

This manuscript was peer reviewed by C. Steelman. The authors gratefully acknowledge C. and E. Weder for allowing this work to take place on their grazing lease. This work was funded by Geoscience BC, Natural Resources Canada Clean Energy Innovation Program, the BC Oil and Gas Commission and the BC Oil and Gas Research and Innovation Society.

References

Appelo, C.A.J. and Postma, D. (2005): Geochemistry, groundwater and pollution, 2nd edition; A.A. Balkema Publishers, Amsterdam, The Netherlands, 649 p.

Berg, R.R. (1975): Capillary pressures in stratigraphic traps; AAPG Bulletin, v. 59, no. 6, p. 939–956.

Brennwald, M.S., Schmidt, M., Oser, J. and Kipfer, R. (2016): A portable and autonomous mass spectrometric system for on-site environmental gas analysis; Environmental Science & Technology, v. 50, issue 24, p. 13455–13463, URL <https://doi.org/10.1021/acs.est.6b03669> [March 2018].

Cahill, A.G., Beckie, R., Ladd, B., Sandl, E., Goetz, M., Chao, J., Soares, J., Manning, C., Chopra, C., Finke, N., Hawthorne, I., Black, A., Mayer, K.U., Crowe, S., Cary, T., Lauer, R., Mayer, B., Allen, A., Kirste, D. and Welch, L. (2019a): Advancing knowledge of gas migration and fugitive gas from energy wells in northeast British Columbia, Canada; Greenhouse Gases: Science and Technology, v. 9, issue 2, p. 134–151, URL <https://doi.org/10.1002/ghg.1856> [November 2019].

Cahill, A.G., Ladd, B., Chao, J., Soares, J., Cary, T., Finke, N., Manning, C., Chopra, C., Hawthorne, I., Forde, O.N., Mayer, K.U., Black, A., Croew, S., Mayer, B., Lauer, R., van Geloven, C., Welch, L. and Beckie, R.D. (2019b): Implementation and operation of a multidisciplinary field investigation involving a subsurface controlled natural gas release, northeastern British Columbia; *in* Geoscience BC Summary of Activities 2018: Energy and Water, Geoscience BC, Report 2019-02, p. 95–103, URL <http://cdn.geosciencebc.com/pdf/SummaryofActivities2018/EW/2016-043_SoA2018_EW_Cahill_ControlledGasRelease.pdf> [October 2019].

Cahill, A.G., Steelman, C.M., Forde, O., Kuloyo, O., Emil Ruff, S., Mayer, B., Mayer, K.U., Strous, M., Ryan, M.C., Cherry, J.A. and Parker, B.L. (2017): Mobility and persistence of methane in groundwater in a controlled-release field experiment; Nature Geoscience, v. 10, no. 4, p. 289–294, URL <https://doi.org/10.1038/ngeo2919> [April 2017].

Cary, T., Lauer, R.M., Innanen, K.A., Beckie, R.D., Cahill, A.G., Chao, J., Soares, J. and Sola, D. (2018): Monitoring methane gas migration in a near surface partially confined aquifer using geophysical methods; American Geophysical Union Fall Meeting, December 10–14, 2018, Washington, DC, Abstract H21I-1743, URL <http://adsabs.harvard.edu/abs/2018AGUFM.H21I1743C> [January 2019].

Chafin, D.T. (1994): Sources and migration pathways of natural gas in near-surface ground water beneath the Animas River valley, Colorado and New Mexico; United States Geological Survey, Water-Resources Investigations Report 94–4006, 56 p., URL <http://pubs.er.usgs.gov/publication/wri944006> [November 2019].

Christensen, T.H., Kjeldsen, P., Bjerg, P.L., Jensen, D.L., Christensen, J.B., Baun, A., Albrechtsen, H. and Heron, G. (2001): Biogeochemistry of landfill leachate plumes; Applied Geochemistry, v. 16, issues 7–8, p. 659–718.

Council of Canadian Academies (2014): Environmental impacts of shale gas extraction in Canada: the expert panel on harnessing science and technology to understand the environmental impacts of shale gas extraction; Council of Canadian Academies, Ottawa, Ontario, 262 p.

DataBC (2019a): Atlas of Canada 1,000,000 national frameworks data – hydrology rivers; BC Ministry of Forests, Lands, Natural Resource Operations and Rural Development and GeoBC, database, URL <https://catalogue.data.gov.bc.ca/dataset/atlas-of-canada-1-000-000-national-frameworks-data-hydrology-rivers> [January 2018].

DataBC (2019b): Digital road atlas (DRA) - master partially-attributed roads; BC Ministry of Forests, Lands, Natural Resource Operations and Rural Development and GeoBC, database, URL <https://catalogue.data.gov.bc.ca/dataset/digital-road-atlas-dra-master-partially-attributed-roads> [January 2018].

DataBC (2019c): Municipalities – Legally defined administrative areas of BC; BC Ministry of Municipal Affairs and Housing, database, URL <https://catalogue.data.gov.bc.ca/dataset/municipalities-legally-defined-administrative-areas-of-bc> [January 2018].

DataBC (2019d): OGC oil and gas regional fields; BC Oil and Gas Commission, database, URL <https://catalogue.data.gov.bc.ca/dataset/9010f337-3a82-4ca0-b2ac-44d72e13ac48> [January 2018].

Dusseault, M., Gray, M. and Nawrocki, P. (2000): Why oilwells leak: cement behavior and long-term consequences; Society of Petroleum Engineers, International Oil and Gas Conference and Exhibition in China, November 7–10, 2000, Beijing, China, conference paper, URL <https://doi.org/10.2118/64733-MS> [May 2018].

Forde, O.N., Cahill, A.G., Beckie, R.D. and Mayer, K.U. (2019a): Barometric-pumping controls fugitive gas emissions from a vadose zone natural gas release; Scientific Reports, v. 9, article no. 14080, 9 p., URL <https://doi.org/10.1038/s41598-019-50426-3> [October 2019].

Forde, O.N., Mayer, K.U. and Hunkeler, D. (2019b): Identification, spatial extent and distribution of fugitive gas migration on the well pad scale; Science of the Total Environment, v. 652, p. 356–366, URL <https://doi.org/10.1016/j.scitotenv.2018.10.217> [February 2019].

IHS Markit (2019): AccuMap™; IHS Markit, mapping, data management and analysis software, URL <https://ihsmarkit.com/products/oil-gas-tools-accumap.html> [January 2018].

Ji, W., Dahmani, A., Ahlfeld, D.P., Lin, J.D. and Hill, E. (1993): Laboratory study of air sparging: air flow visualization; Ground Water Monitoring & Remediation, v. 13, issue 4, p. 115–126, URL <https://doi.org/10.1111/j.1745-6592.1993.tb00455.x> [January 2019].

Johnson, R.L., Johnson, P.C., Amerson, I.L., Johnson, T.L., Bruce, C.L., Leeson, A. and Vogel, C.M. (2001): Diagnostic tools for integrated in situ air sparging pilot tests; Bioremediation Journal, v. 5, issue 4, p. 283–298, URL <https://doi.org/10.1080/20018891079339> [January 2019].

Kljun, N., Calanca, P., Rotach, M.W. and Schmid, H.P. (2015): A simple two-dimensional parameterisation for Flux Footprint Prediction (FFP); Geoscientific Model Development, v. 8, p. 3695–3713, URL <https://doi.org/10.5194/gmd-8-3695-2015> [November 2018].

Kormann, R. and Meixner, F.X. (2001): An analytical footprint model for non-neutral stratification; Boundary-Layer Meteorology, v. 99, issue 2, p. 207–224, URL <https://doi.org/10.1023/A:1018991015119> [November 2018].

Lovley, D.R. and Chapelle, F.H. (1995): Deep subsurface microbial processes; Reviews of Geophysics, v. 33, issue 3, p. 365–381.

Mercer, J.W. and Cohen, R.M. (1990): A review of immiscible fluids in the subsurface: properties, models, characterization and remediation; Journal of Contaminant Hydrology, v. 6, issue 2, p. 107–163, URL <https://doi.org/10.1016/0169-7722(90)90043-G> [September 2019].

Parker, J.C. (1989): Multiphase flow and transport in porous-media; Reviews of Geophysics, v. 27, issue 3, p. 311–328.